

PAPER • OPEN ACCESS

Effect of Steel Slag on Crystallization and Bending Strength of Glass Ceramics Based on Blast Furnace Slag

To cite this article: X M Shen *et al* 2019 *IOP Conf. Ser.: Earth Environ. Sci.* **281** 012033

View the [article online](#) for updates and enhancements.



IOP | ebooks™

Bringing you innovative digital publishing with leading voices to create your essential collection of books in STEM research.

Start exploring the **collection** - download the first chapter of every title for free.

Effect of Steel Slag on Crystallization and Bending Strength of Glass Ceramics Based on Blast Furnace Slag

X M Shen^{1,*}, H T Zhao¹, X R Wu², F B Cao², P Wang² and L S Li¹

¹Key Laboratory of Metallurgical Emission Reduction & Resources Recycling of Ministry of Education, Anhui University of Technology, Ma'anshan, 243002, China

²Anhui Province Key Laboratory of Metallurgy Engineering & Resources Recycling, Anhui University of Technology, Ma'anshan, 243002, China

* xxxmx@126.com

Abstract. The glass ceramics based on steel slag and blast furnace slag presented light-khaki color to deep-brown color with increasing content of steel slag. The major crystalline phase is gehlenite ($\text{Ca}_2\text{Al}_2\text{SiO}_7$) with minor akermanite phase ($\text{Ca}_2\text{MgSi}_2\text{O}_7$) for all the samples. Decreasing Al_2O_3 and increasing Fe_2O_3 in the samples increased glass viscosity, and decreasing SiO_2 decreased the amount of liquid phase. Both the above effects result in the increasing optimum sintering temperature. The grain size and amount of crystalline phase were increased with content of steel slag. The bending strength of the samples first increases with content of steel slag up to a maximum 90 MPa, then decreases. The bulk density of the samples decreases with increasing content of steel slag, from 2.76 g/cm^3 to 2.60 g/cm^3 , owing to lower content of glass phase during sintering process. The samples exhibit good chemical resistance, and the weight loss values in alkali are lower than those in acid. Therefore, the glass ceramics based on steel slag and blast furnace slag may have great potential for applications as building decorative materials, and it provides a promising way for the utilization of steel slag.

1. Introduction

Steel slag is a kind of intractable metallurgical waste. Owing to highly variable chemical composition depending on the raw materials and production process, difficulty in grinding and higher amount of P/S, large utilization of steel slag is not that easy. Nowadays, steel slag is mainly utilized in buliding materials [1-5]. Steel slag contains useful components, such as calcium oxide, silicon dioxide, magnesium oxide and so on, which are important components of glass ceramics.

In recent years, blast furnace slag [6, 7], coal combustion ash [8, 9], fly ash and filter dusts from waste incinerators [10-12], mud from metal hydrometallurgy [13, 14], different types of sludge [15, 16] and other metallurgical wastes [17, 18] have been used for preparation of glass ceramics. However, there are only a few reports on the use of steel slag for glass ceramics preparation, and due to relatively lower content of silicon dioxide, other raw materials must be added for preparing glass ceramics. G.A. Khater [19] has reported that 57 % steel slag, quartz sand, clay, dolomite and limestone were successfully used for preparation of glass ceramics, and increasing content of bustamite phase results in an increased bulk crystallinity and increasing fayalite phase results in decreased crystallinity. Liquid-liquid mixing method was proposed by Zhang et al. [20] to prepare glass ceramics from molten steel slag and chemical additives, and the proportion of steel slag in the melt was 50 wt.%. Their microstructure and crystallized phase were also analyzed. Above studies have mainly focused on the



use of steel slag and other chemical materials for preparation of glass ceramics which is not considered economically feasible, while studies on the use of steel slag and other wastes for glass ceramics preparation have not been reported yet. In this paper, glass ceramics were prepared by steel slag and blast furnace slag, and the effect of steel slag on crystallization and bending strength of the samples were investigated.

2. Experimental procedure

2.1. Preparation of glass ceramics

Glass ceramics based on steel slag and blast furnace slag were prepared by a single sintering process. Steel slag and blast furnace slag used in this work were obtained from Maanshan Iron and Steel Co. Ltd. located in east-central China, and steel slag used is a kind of air quenched steel slag, which is obtained by a high-speed air flow impacting the falling molten slag. Chemical compositions of air quenched steel slag and blast furnace slag are shown in Table 1, respectively.

Table 1. Chemical composition of air quenched steel slag and blast furnace slag. (wt%)

Component	SiO ₂	CaO	Al ₂ O ₃	MgO	Fe ₂ O ₃	FeO	TiO ₂	MnO	K ₂ O	Na ₂ O
Air quenched steel slag	11.26	42.59	2.01	8.22	19.59	9.85	0.837	2.51	0.011	0.117
Blast furnace slag	32.77	40.48	17.19	6.59	0.27	0.19	0.724	0.316	0.293	0.309

The steel slag and blast furnace slag were dried at 353 K for 24 h before use, and then were crushed to pass 200 mesh and mixed at ratios of 1:9, 2:8, 3:7, 4:6 and 5:5 by weight, respectively. After adding fluxing agent and binding agent, the mixture was pressed at 30 MPa and then shaped in a steel die. Finally, the compacts were heated at 673 K for 1.5 h to remove organic binding agent, and sintered at different temperature for 3 h. The obtained samples were denoted by A, B, C, D and E.

2.2. Characterization

The chemical composition of the samples was determined by ARL Advant X Intellipower 3600 X-ray fluorescence (XRF). The structure of the samples was measured by Bruker AXS-D8 Advance X-ray powder diffraction (XRD). The morphology of the samples was observed by S4300 scanning electron microscope (SEM). The bending strength was tested by three point bending method. The chemical resistance was examined in acid and alkali solutions. The samples were immersed respectively in H₂SO₄ (1 mass%) solution and NaOH (1 mass%) solution for 24 h, then, washed with deionized water, dried at 393 K for 12 h and weighed. The bulk densities of the samples were measured by the Archimedes method using water.

3. Results and discussion

Figure 1 shows the relationship between the optimum sintering temperature of the samples and content of steel slag. The optimum sintering temperature is determined by XRD patterns, density and appearance of the samples together, as shown in Table 2. The samples present light-khaki color to deep-brown color with increasing content of steel slag and samples sintering at optimum temperature possess smooth surface and high gloss. However, samples sintering below optimum temperature present rough surface with small bumps. With the increase of sintering temperature, the surface of the samples became smooth, and then, the samples presented broad and weak XRD peaks, because more glass phase appeared. The samples showed an overfiring behaviour when sintered above optimum temperature about 25 K. From Figure 1, it can be seen that the optimum sintering temperature of the samples increases with the increase of steel slag. On the one hand, Al₂O₃ content in the samples, which hinders the process of crystallization [21], decreases sharply with increasing steel slag, and the glass viscosity increases with increasing crystalline content. On the other hand, the content of Fe₂O₃ increases rapidly with increasing steel slag, which promotes the crystallization [22], and thus, increases the glass viscosity. In addition, the content of SiO₂ decreases with increasing steel slag

which decreases the amount of liquid phase. The sintering process depends mainly on liquid phase, and the amount of liquid phase and the viscosity of the liquid depend mainly on the sintering temperature. Therefore, both the above effects result in the increasing optimum sintering temperature.

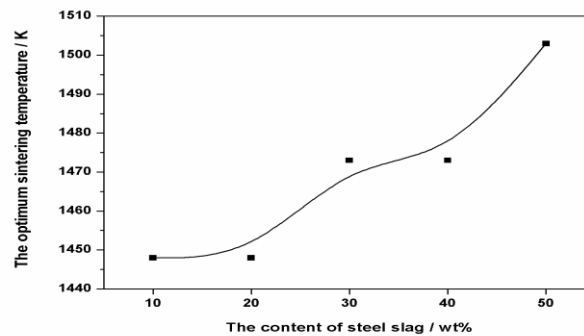


Figure 1. The relationship between the optimum sintering temperature of the samples and content of steel slag.

Table 2. Density and appearance of the samples sintering at different temperatures.

Number	Sintering temperature (K)	Density (g cm^{-3})	Appearance of the samples
A	1423	2.73	light khaki color, rough surface with bumps
	1448	2.76	light khaki color, smooth surface, high gloss
	1473	—	light khaki color, more glass phase, overfiring
	1503	—	—
B	1423	2.71	khaki colour, rough surface with bumps
	1448	2.74	khaki colour, smooth surface, high gloss
	1473	—	khaki colour, more glass phase, overfiring
	1503	—	—
C	1423	2.65	light brown colour, rough surface with many bumps
	1448	2.67	light brown colour, relatively smooth surface
	1473	2.69	light brown colour, smooth surface, high gloss
	1503	—	light brown colour, more glass phase, overfiring
D	1423	2.64	brown colour, rough surface with many bumps
	1448	2.65	brown colour, relatively smooth surface
	1473	2.65	brown colour, smooth surface, high gloss
	1503	—	brown colour, more glass phase, overfiring
E	1423	2.57	deep brown colour, rough surface with many bumps
	1448	2.59	deep brown colour, rough surface with less bumps
	1473	2.59	deep brown colour, relatively smooth surface
	1503	2.6	deep brown colour, smooth surface, high gloss

A, B, C, D and E samples obtained at optimum sintering temperature, respectively, were measured by X-ray diffraction, and the patterns show that the major crystalline phase is gehlenite ($\text{Ca}_2\text{Al}_2\text{SiO}_7$) with minor akermanite phase ($\text{Ca}_2\text{MgSi}_2\text{O}_7$) for all of the samples. In order to investigate the effect of steel slag on crystallization of samples under the same sintering conditions, the samples were sintered at 1448 K for 3 h. The XRD patterns of A and C samples were shown in Figure 2, and gehlenite with minor akermanite peaks were observed for the samples. Note that, the diffraction intensity of C sample is obviously lower than that of A sample. This is because that, as the content of steel slag increases, the optimum sintering temperature of the samples increases, as shown in Figure 1. Although both decrease of Al_2O_3 content and increase of Fe_2O_3 content are beneficial to crystallization of samples, thermodynamics condition is not fully satisfied. That is to say, sintering temperature of 1448 K is lower for C sample.

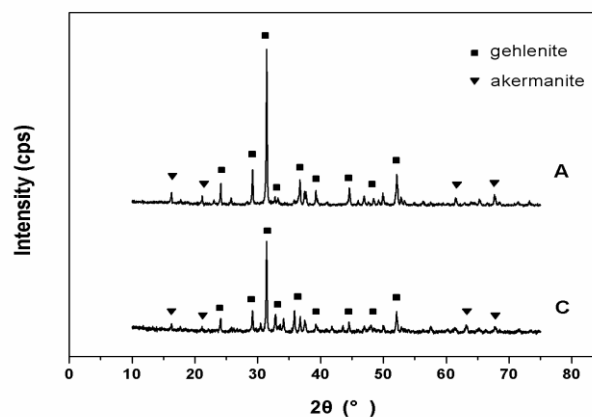


Figure 2. The XRD patterns of A and C samples sintered at 1448 K for 3 h.

The SEM images of A, B and C samples obtained at optimum sintering temperature are shown in Figure. 3(a), Figure. 3(b) and Figure. 3(c), respectively. As can be seen in Figure. 3(a), the small grains with the size of 0.5~1 μm were randomly distributed in A sample. For B sample, the amount of crystalline phase was increased, and besides dispersed small grains, a few irregular large grains were observed in Figure. 3(b) indicating that steel slag addition can accelerate grain growth of the sample. From Figure. 3(c), it can be seen that most of small grains disappeared and large grains were significantly increased. The rapid growth of grains was owing to obvious content changes of Al_2O_3 and Fe_2O_3 .

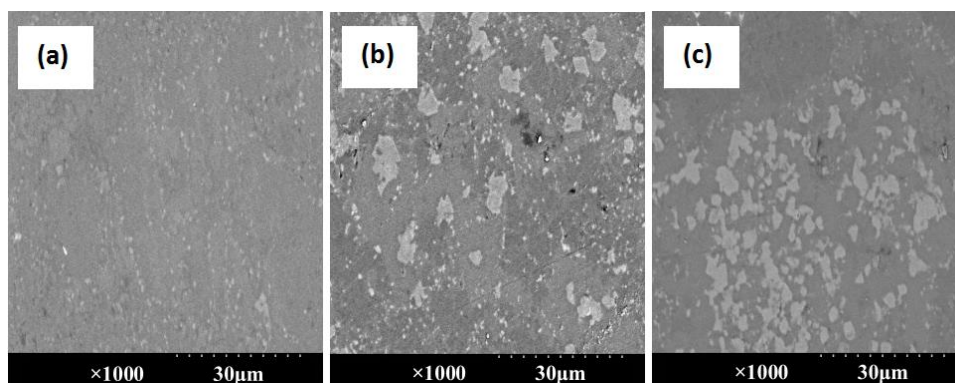


Figure 3. The SEM images of A, B and C samples obtained at optimum sintering temperature.

Figure 4 shows the relationship between bending strength of the samples and the content of steel slag. As can be seen in the figure, the bending strength of the samples first increases with content of steel slag up to a maximum, then decreases. At lower content of steel slag (10 %), the bending strength

of the sample is 85 MPa. When the content of steel slag is 20 %, the bending strength reaches its maximum value 90 MPa, due to larger amount of crystalline phase as shown in Figure 3. The bending strength of the samples then decreases with continuous increase of steel slag (over 20 %), and is down to 73 MPa as the content of steel slag is 50 %. The amount of crystalline phase in samples with higher content of steel slag is larger than that with lower content of steel slag, which is beneficial to bending strength. However, more large grains in samples with higher content of steel slag result in decreasing mechanical properties.

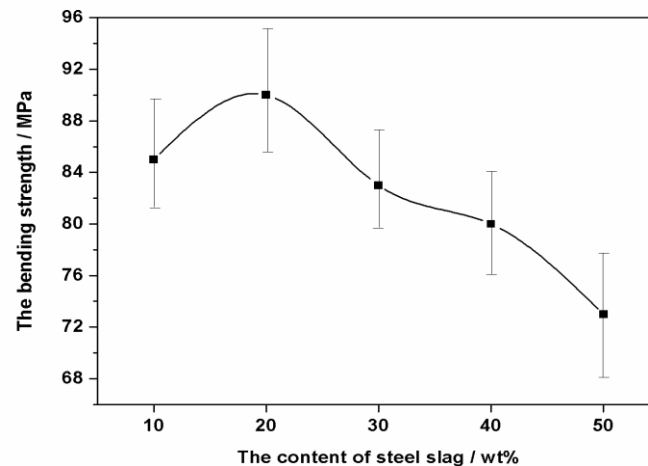


Figure 4. The relationship between bending strength of the samples and the content of steel slag.

The chemical resistance and bulk density of the samples are shown in Table 3. The samples exhibit good chemical resistance, and the weight loss values in alkali are lower than those in acid. The bulk density of the samples decreases with increasing content of steel slag, from 2.76 g/cm³ to 2.60 g/cm³. The reason may be due to lower content of glass phase during sintering process in samples with higher content of steel slag, which is against densification process. Therefore, the bulk density of the samples decreases.

Table 3. The chemical resistance and bulk density of the samples

Number	A	B	C	D	E
Weight loss in acid (%)	1.24	1.04	0.98	1.29	1.37
Weight loss in alkali (%)	0.86	0.81	0.88	0.95	1.00
Bulk density (g cm ⁻³)	2.76	2.74	2.69	2.65	2.60

4. Conclusion

The glass ceramics based on steel slag and blast furnace slag presented light-khaki color to deep-brown color with increasing content of steel slag, and the samples were gehlenite with minor akermanite. Decreasing Al₂O₃ and increasing Fe₂O₃ in the samples increased glass viscosity, and decreasing SiO₂ decreased the amount of liquid phase. Both the above effects result in the increasing optimum sintering temperature. Due to larger amount of crystalline phase, the bending strength of 20% steel slag sample reached 90Mpa. The ceramics exhibit good chemical resistance, and the weight loss values in alkali are lower than those in acid. The ceramics may have great potential for applications as building decorative materials.

Acknowledgments

We are thankful for the financial support provided by AnHui Provincial Natural Science Foundation (No. 1708085ME119), University Science Research Project of AnHui Province (KJ2017A050, KJ2018A0067) and Anhui innovation team project of new technology in materialization of metallurgical solid wastes.

References

- [1] Tsakiridis P E, Papadimitriou G D, Tsivilis S and Koroneos C 2008 *J. Hazard. Mater.* **152** 805
- [2] Altun I A and Yilmaz I 2002 *Cem. Concr. Res.* **32** 1247
- [3] Wu S, Xue Y, Ye Q and Chen Y 2007 *Build. Environ.* **42** 2580
- [4] Wu X, Zhu H, Hou X and Li H 1999 *Cem. Concr. Res.* **29** 1103
- [5] Maslehuddin M, Sharif A M, Shameem M, Ibrahim M and Barry M S 2003 *Constr. Build. Mater.* **17** 105
- [6] Liu H Y, Lu H X, Chen D L, Wang H L, Xu H L and Zhang R 2009 *Ceram. Int.* **35** 3181
- [7] Das B, Prakash S, Reddy P S R and Misra V N 2007 *Resour. Conserv. Recy.* **50** 40
- [8] Erol M, Küçükbayrak S and Ersoy-Mericboyu A 2008 *J. Hazard. Mater.* **153** 418
- [9] Peng F, Liang K and Hu A 2005 *Fuel*. **84** 341
- [10] Rozenstrauha I, Bajare D, Cimdins R, Berzina L, Bossert J and Boccaccini A R 2006 *Ceram. Int.* **32** 115
- [11] Park Y J and Heo J 2004 *Waste Manage.* **24** 825
- [12] Qian G, Song Y, Zhang C, Xia Y, Zhang H and Chui P 2006 *Waste Manage.* **26** 1462
- [13] Yang J, Zhang D, Hou J, He B and Xiao B 2008 *Ceram. Int.* **34** 125
- [14] Peng F, Liang K M, Shao H and Hu A 2005 *Chemosphere*. **59** 899
- [15] Toya T, Kameshima Y, Nakajima A and Okada K 2006 *Ceram. Int.* **32** 789
- [16] Toya T, Nakamura A, Kameshima Y, Nakajima A and Okada K 2007 *Ceram. Int.* **33** 573
- [17] Khater G A 2010 *J. Non-Cryst. Solids*. **356** 3066
- [18] Bernardo E, Castellan R and Hreglich S 2007 *Ceram. Int.* **33** 27
- [19] Khater G A 2002 *Ceram. Int.* **28** 59
- [20] Zhang K, Liu J, Liu W and Yang J 2011 *Chemosphere*. **85** 689
- [21] Liu C, Zhang Y, Shi P and Jiang M 2007 *Rare Metal Mat. Eng.* **36** 306
- [22] Rezvani M, Eftekhari-Yekta B, Solati-Hashjin M and Marghussian V K 2005 *Ceram. Int.* **31** 75